journal of the mechanical behavior of biomedical materials 139 (2023) 105672

Contents lists available at ScienceDirect

Journal of the Mechanical Behavior of Biomedical Materials

journal homepage: www.elsevier.com/locate/jmbbm

Age-dependent mechanical properties of tail tendons in wild-type and mimecan gene-knockout mice – A preliminary study

C. Boote [a,b,c], Q. Ma [a], K.L. Goh [a,c,d,*]

[a] School of Optometry and Vision Sciences, Cardiff University, Cardiff, UK
[b] Department of Biomedical Engineering, National University of Singapore, Singapore
[c] Newcastle Research and Innovation Institute (NewRIIS), Singapore
[d] Faculty of Science, Agriculture and Engineering, Newcastle University, Newcastle Upon Tyne, UK

ARTICLE INFO

Keywords:
Elasticity
Fracture
Tendon diameter
Mimecan
Osteoglycin

ABSTRACT

Mimecan, or osteoglycin, belongs to the family of small leucine-rich proteoglycans. In connective tissues mimecan is implicated in the development and maintenance of normal collagen fibrillar organization. Since collagen fibrils are responsible for tissue reinforcement, the absence of mimecan could lead to abnormal tissue mechanical properties. Here, we carried out a preliminary investigation of possible changes in the mechanical properties of tendons in mice lacking a functional mimecan gene, as a function of age. Tail tendons were dissected from mimecan gene knockout (KO) and wild type (WT) mice at ages 1, 4 and 8 months and mechanical properties evaluated using a microtensile testing equipment. Mimecan gene knockout resulted in changes in tendon elasticity- and fracture-related properties. While tendons of WT mice exhibited enhanced mechanical properties with increasing age, this trend was notably attenuated in mimecan KO tendons, with the exception of fracture strain. When genotype and age were considered as cross factors, the diminution in the mechanical properties of mimecan KO tendons was significant for yield strength, modulus and fracture strength. This effect appeared to affect the mice at 4 month old. These preliminary results suggest that mimecan may have a role in regulating age-dependent mechanical function in mouse tail tendon.

1. Introduction

Mimecan, also known as osteoglycin, belongs to the family of small leucine-rich proteoglycans (SLRPs) (Tasheva, 2002, Tasheva et al., 2002) - extracellular matrix (ECM) components of connective tissues. Each proteoglycan (PG) macromolecule features a protein core (comprising leucine-rich repeats), 'flanked' by cysteine-rich clusters at the N-terminal, and these clusters are covalently bonded with glycosaminoglycan (GAG) side chains (Schaefer and Iozzo, 2008; Iozzo and Schaefer, 2015). There are five classes of SLRPs, categorised according to the cysteine-rich clusters and C-terminal repeats, chromosome organization and protein and gene homology - mimecan is a class III SLRP (Iozzo and Schaefer, 2015). Mimecan PGs are attached with keratan sulfate (KS), which is a glycosaminoglycan polysaccharide (Funderburgh et al., 1997; Tasheva, 2002, Tasheva et al., 2002). The presence of GAG sulfate groups yields a net negative charge (Casroro et al., 1988) which facilitates binding of water molecules and is largely responsible for the ECM swelling pressure (Casroro et al., 1988).

SLRPs have regulatory roles in collagen fibril assembly, development and organisational homeostasis (Schaefer and Iozzo, 2008; Chen and Birk, 2013; Dunkman et al., 2013; Iozzo and Schaefer, 2015), however how mimecan performs these roles is still not fully understood. Collagen fibrils facilitate the mechanical stability of connective tissues by providing reinforcement to the weaker ground substance (Hukins, 1982, Goh et al., 2005; Goh et al., 2007). Importantly, Tasheva and co-workers found that the mean fibril size and the range of fibril sizes in dorsal skin differed appreciably between one year-old mimecan-KO and wild-type (WT) mice (Tasheva et al., 2002). The fracture strength of KO dorsal skin was also lower compared to that of WT skin (Tasheva et al., 2002), suggesting that mimecan may modulate tissue mechanics at the ECM ultrastructural level.

Tendon is a connective tissue comprising highly parallel collagen fibrous structures reinforcing a hydrated PG-rich ECM (Goh et al., 2003; Goh et al., 2005; Goh et al., 2007; Goh et al., 2014). The structure of tendon collagen is hierarchical, with the following architectural levels from largest to smallest: fascicle, fibril, microfibril and tropocollagen

* Corresponding author. School of Optometry and Vision Sciences, Cardiff University, Cardiff, UK.
E-mail address: kheng-lim.goh@ncl.ac.uk (K.L. Goh).

https://doi.org/10.1016/j.jmbbm.2023.105672
Received 3 September 2022; Received in revised form 3 January 2023; Accepted 7 January 2023
Available online 10 January 2023

molecule (Goh et al., 2003; Goh et al., 2005; Goh et al., 2007; Goh et al., 2014). As an organism ages, it experiences diminished physiological function and increased vulnerability to disease (Lopez-Otin et al., 2013). Some age-dependent changes occur at macroscopic length scale, while others (e.g. collagen fibril diameter) manifest at sub-micron length scales. Age-related studies on tendon mechanics have demonstrated variation in strength and stiffness (Goh et al., 2008) as well as resilient energy and fracture toughness (Goh et al., 2012) with increasing age. These variations have been attributed to changes in collagen structure (Parry et al., 1978) and cross-links (Bailey et al., 1998). Mouse gene knockout models have provided valuable insight into the role of SLRPs in regulating tendon development, maturation and function. Double knockout of biglycan and decorin in mice results in tendon weakening and associated alterations in collagen fibril structure (Gordon et al., 2015) while biglycan/fibromodulin null animals exhibit ectopic tendon ossification and resulting mechanical function impairment (Kilts et al., 2009). Similarly, mice lacking expression of lumican and fibromodulin demonstrate age-dependent joint laxity and impaired tendon integrity resulting from disrupted collagen fibrillogenesis (Ezura et al., 2000; Jepsen et al., 2002). However, up to now similar insight into the potential role of mimecan in tendon mechanical function has remained elusive.

The purpose of the present study is to assess the role of mimecan on tendon mechanical properties using a mimecan knockout mouse model, and to investigate its possible modulation with age. Here we report a preliminary study on the elasticity and fracture properties of tail tendons in mimecan-knockout and wild-type C57BL/6 mice in three different age groups.

2. Materials and methods

2.1. Mimecan-deficient mice

The authors were provided with tendons from the tails of mimecan-deficient (KO) and wild type (WT) C57BL/6 male mice (11 WT, and 11 KO), courtesy of Prof Gary W Conrad (Division of Biology, Kansas State University, Manhattan, KS, USA). The mice were divided into the following age groups: 1 month old (mo) (N = 3), 4 mo (N = 3) and 8 mo (N = 5). The husbandry and maintenance of mimecan-deficient mouse lines has been described previously (Tasheva et al., 2002). In brief, the KO and WT mice were housed in the animal care facility at the Division of Biology, Kansas State University, according to NIH guidelines (NIH publication No. 86–23,1985) and IACUC approved protocols. The animals were euthanized by cervical dislocation. Animal handling was carried out in accordance with the ARVO Statement for the Use of Animals in Ophthalmic and Vision Research. Immediately following euthanization, the tail of each mouse was removed and wrapped in plastic film to limit dehydration, frozen in liquid nitrogen, and shipped on dry ice to Cardiff University for testing.

Prior to testing, each tail was dissected under magnification. First the skin was removed from the tail to expose the tendons. Each tendon fascicle was then isolated from the tail by sliding it out along the tail with minimum force, so as to minimise any damage. For each mouse, 12 segments (each 7 mm long) from randomly selected tendon fascicles were prepared.

2.2. Micromechanical testing

Fig. 1 (a) shows the custom-designed small scale horizontal tensile test frame device that was used in this study (Goh et al., 2008; Goh et al., 2010; Goh et al., 2012). The restoring force, P, generated in the sample and relative displacement, x, between the pair of grip plates were recorded using a load cell (450 g linear range) and a displacement transducer, respectively.

The procedure for mechanical testing of soft tissues with micrometer-scale dimensions is described in detail elsewhere (Goh et al., 2008; Goh et al., 2010; Goh et al., 2012). In brief, a small scale horizontal tensile test frame device was used to stretch each segment at a strain-rate of 0.067 mm/s from a slightly slackened state until rupture. The ends of each sample were fixed to a thin aluminium rectangular frame using cyanoacrylate adhesive (Fig. 1 (b)). Before stretching the tendon, the two sides of the template in parallel to the tendon were cut away. Throughout the experiment each sample was kept hydrated by submerging in phosphate buffer saline (PBS) solution (pH 7.2) in a petri dish (Fig. 1 (c)).

2.3. Data processing

Data of load versus extension for each specimen were evaluated to obtain stress versus strain data to determine the material (mechanical) properties. Strain (ε) was determined using $\varepsilon = x/L$ where x is extension (section 2.2) and L is the nominal length of the sample found by measuring the grip-to-grip distance after straightening the tendons to remove the 200 microscopic crimps (Goh et al., 2008; Goh et al., 2010; Goh et al., 2012). Stress (σ) was calculated using $\sigma = F/A$, where F is the force measured by the load cell and A is the nominal mean cross-sectional area of the tendon, which we assumed to be circular (Goh et al., 2008; Goh et al., 2010; Goh et al., 2012). A was found by measuring the fascicle diameters at five different locations along the tendon using a digital image of the tendon, captured under a transmission light microscope using the software ImageJ (Goh et al., 2008; Goh et al., 2010; Goh et al., 2012). The mean diameter (d) was then

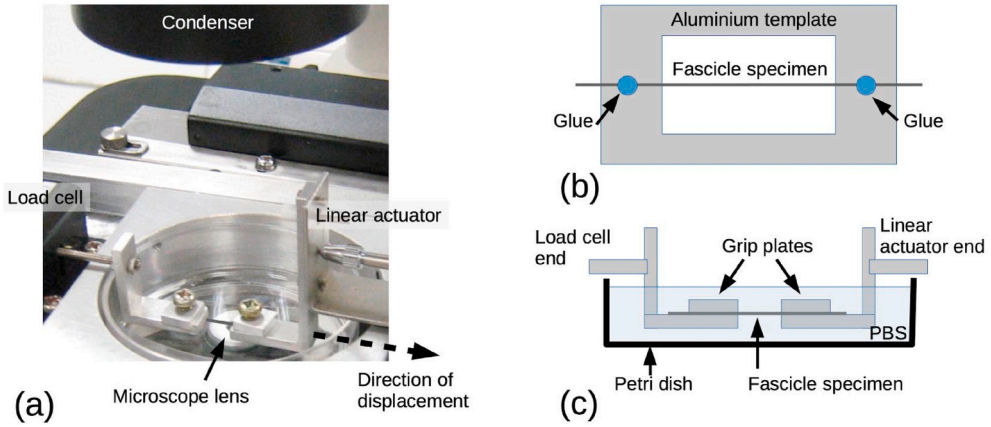

Fig. 1. Micromechanical testing. (a) Set-up of the micromechanical test system. (b) Schematic of template for holding fascicle specimen temporarily, while securing the fascicle to the grip plates. (c) Schematic of the horizontal testing approach. PBS was used to keep the fascicle hydrated during the test.

determined for each sample and A was subsequently calculated using $A = (d/2)^2$.

The stress-strain curves featured an S-shape profile typical of collagen fascicles and described elsewhere (Goh et al., 2008; Goh et al., 2010; Goh et al., 2012). The determination of the mechanical parameters from the stress-strain curve followed our previous studies (Goh et al., 2008; Goh et al., 2010; Goh et al., 2012). The tendon fracture strength was identified with the maximum stress prior to rupture; the tendon fracture strain was identified with the strain at maximum stress. To determine the tensile modulus of each age group, a fifth-order polynomial equation was used to fit the stress-strain data points (from each sample) from $\varepsilon = 0$ to the fracture strain using a least-squares method (lower orders were not adequate for fitting the data.) Given that the region from $\varepsilon = 0$ to the fracture strain was non-linear, we selected the point of inflexion on the fitted curve to calculate the gradient and thus derive the tensile modulus. To estimate the yield strength and yield strain, we identified the occurrence of yield in the tendon with the point of inflexion (Goh et al., 2008; Goh et al., 2010; Goh et al., 2012). The strain energy density to resilience, otherwise known as the resilience, refers to the amount of energy per unit volume absorbable by the deforming until the yield point. The resilience was determined from the area under the stress-strain curve from the origin to

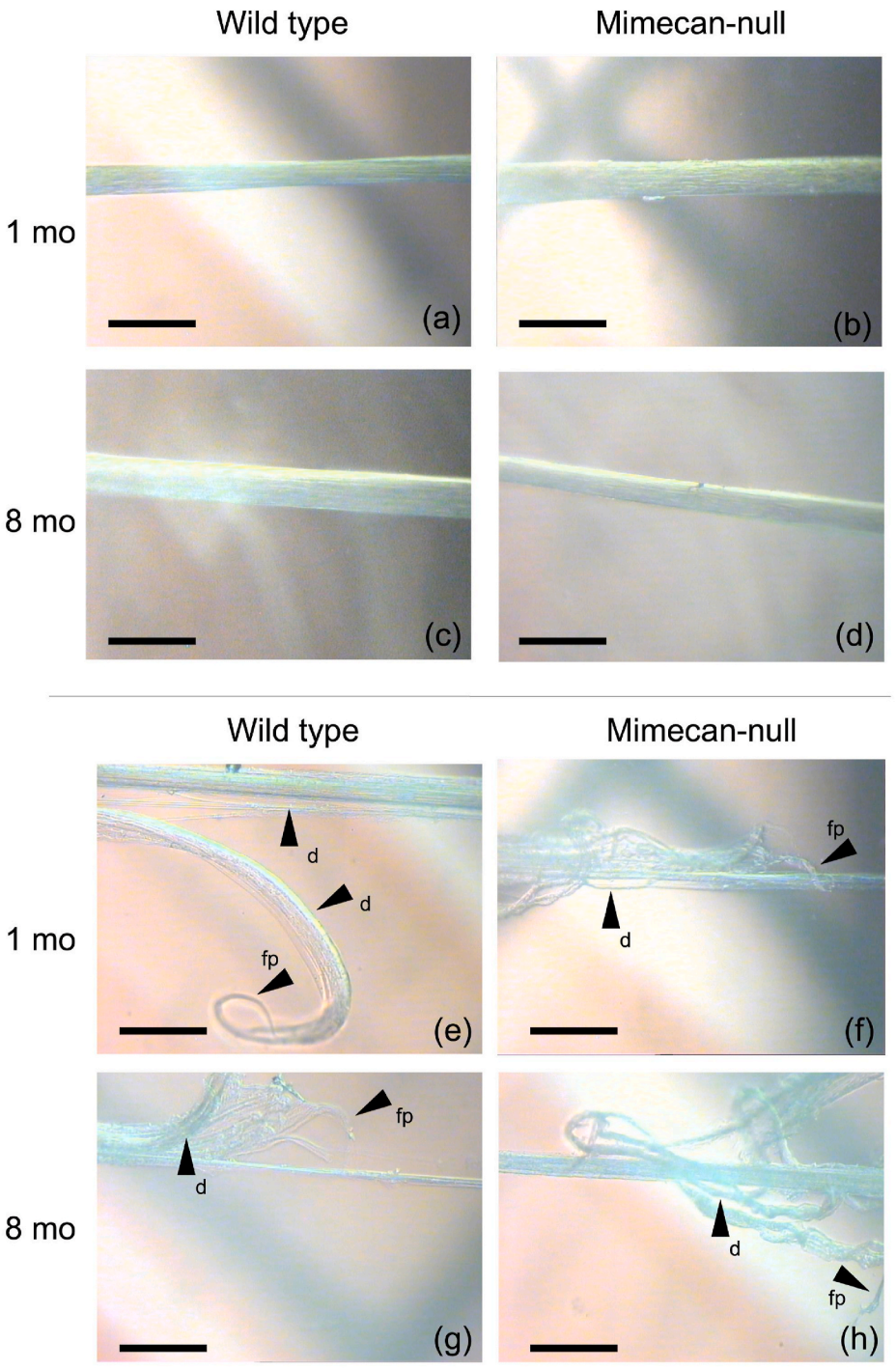

Fig. 2. Morphological features of tendon fascicles. Panels (a)–(d) show the fascicles before mechanical testing. Panels (e)–(h) show the fractured fascicles after mechanical testing. Scale bar represents 20 μm d and fp denote defibrillation and fibre pull-out, respectively.

the yield strain. The strain energy density to failure, otherwise known as fracture toughness, refers to the amount of energy per unit volume absorbable by the deforming tissue until the tendon ruptures into two. The fracture toughness was determined from the area under the stress-strain curve from the origin to the end point (i.e. maximum strain), using the trapezium rule.

2.4. Statistical analysis

Our hypothesis was that the elasticity and fracture characteristics of mimecan-null tendons differ from native tendons, and that this is modulated by the presence of aging. Statistical analysis was performed using JMP software (JMP 17 for Windows, SAS institute, Cary, NC, USA). To compare mechanical parameters at different ages within each genotype, a mixed-effects model followed by Tukey's multiple comparisons test was used. The mixed effects model leveraged the 12 randomly selected tendons from each individual mouse tail and treated them as repeat measures in the model. Genotype and age were considered crossed factors with repeat measure a nested factor within each animal. The analysis considered both main-effects and interactions (full factorial). Animal number was considered a random factor. $P < 0.05$ was considered statistically significant. In the resulting table and graphs, results are reported as mean ± standard deviation (of population).

3. Results

3.1. Stress-strain profiles

Fig. 2 (a - d) shows the fascicle specimens prior to mechanical testing. These specimens were derived from 1 mo to 8 mo WT and KO mice. The micrographs show the specimen in a stretched state, following the removal of the macroscopic crimp pattern, just before loading commenced. Highly parallel streaks, visible along the axis of the fascicle, were associated with collagen fibres. These fibres appeared to be tightly packed and opaque. No appreciable variation in the features was observed between the specimens of WT and KO mice. Overall, there was no significant variation in the thickness of the tendons for WT versus KO or with respect to age. The average thickness of the tendon was 116 ± 28 μm (WT) and 122 ± 32 μm (KO), in good order of magnitude agreement with reports from previous studies (Goh et al., 2018).

Fig. 2(e–h) show the fracture morphologies of the fascicle specimens from the WT and KO mice at 1 mo and 8 mo. Failure modes, namely defibrillation of collagen fibre bundles, fibre pull-out and fibre fracture, were observed in all cases. No appreciable variation was observed in the fracture morphologies between the specimens of WT and KO mice.

Fig. 3 shows graphs of stress versus strain for fascicles (at 1 mo and 8 mo), plotted for WT and KO mice, respectively. In all cases, it was observed that the curve profiles were somewhat similar in relation to the toe region having a low modulus at small strain (suggesting that a high proportion of the collagen fibrils were still in the crimped state), near-linear stress-strain region as the fascicle was stretched (suggesting that the collagen fibrils had straightened), a stress-plateau (i.e. strain-softening) region at high strain, followed by rapidly decreasing stress as the fascicle ruptured. Interestingly, the WT fascicles (Fig. 3(a)) featured an extended stress-plateau region as compared to KO fascicles (Fig. 3(b)), most prominently in the younger (1 mo) mice.

3.2. Elasticity properties

The mean results of the elasticity-related mechanical properties for each age point and genotype are listed in Table 1, and are displayed graphically in Fig. 4.

Graphs displaying the effects of age on WT and KO elasticity properties are shown in Fig. 4 (a, d, g). For WT mice (circles), significantly enhanced tendon yield strength, modulus and resilience were observed in older age groups compare to 1 mo animals. For KO mice (squares), this trend was attenuated across all three parameters.

The overall effect of mimecan removal (i.e. pooling all tendon samples at all ages within each genotype) is seen in Fig. 4 (b, e, h), where the mean value shows a consistent decrease across all three elasticity parameters for KO mice compared to WT animals. However, when considering genotype and age as crossed factors, this reduction only met the threshold for statistical significance in the case of yield strength (Fig. 4(b)) and modulus (Fig. 4(e)).

The effect of genotype is broken down by age group and statistically

Table 1
Summary of mechanical properties in mimecan-null (KO) versus wild-type (WT) mice as found in this study. The values under columns WT and KO refer to mean and standard deviation.

Parameter	Age	WT	KO
Modulus (MPa)	1 mo	346.9 ± 170.4	365.0 ± 203.4
	4 mo	518.2 ± 156.4	399.4 ± 157.6
	8 mo	421.0 ± 147.5	398.3 ± 152.5
Yield Strength (MPa)	1 mo	11.4 ± 5.5	12.1 ± 6.1
	4 mo	20.7 ± 6.4	15.4 ± 5.9
	8 mo	19.4 ± 7.3	16.9 ± 7.0
Yield Strain	1 mo	0.060 ± 0.019	0.060 ± 0.020
	4 mo	0.060 ± 0.014	0.059 ± 0.014
	8 mo	0.065 ± 0.017	0.059 ± 0.017
Fracture Strength (MPa)	1 mo	28.4 ± 16.6	29.1 ± 17.6
	4 mo	58.7 ± 19.8	42.4 ± 17.3
	8 mo	52.0 ± 20.8	45.4 ± 18.9
Fracture Strain	1 mo	0.165 ± 0.034	0.150 ± 0.027
	4 mo	0.208 ± 0.028	0.193 ± 0.040
	8 mo	0.199 ± 0.031	0.184 ± 0.037
Resilience (kJ/m^3)	1 mo	0.219 ± 0.137	0.223 ± 0.115
	4 mo	0.461 ± 0.185	0.333 ± 0.159
	8 mo	0.498 ± 0.237	0.403 ± 0.228
Fracture Toughness (kJ/m^3)	1 mo	3.1 ± 2.7	2.6 ± 2.1
	4 mo	7.6 ± 3.5	5.1 ± 2.6
	8 mo	6.1 ± 3.0	5.1 ± 3.0

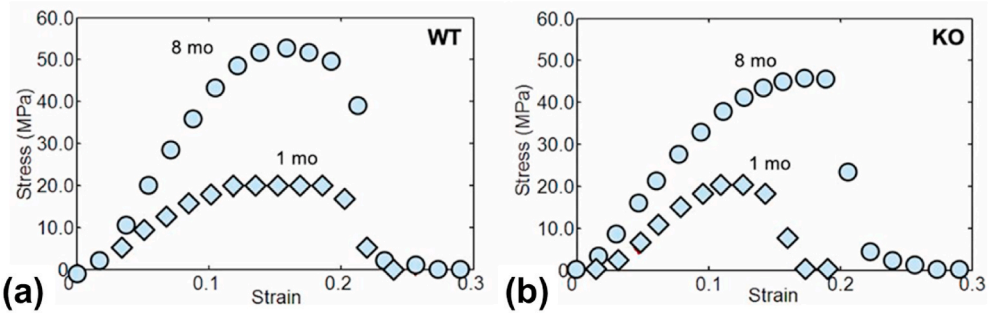

Fig. 3. Graphs of representative stress–strain curves of tendon fascicles from (a) wild-type (WT) and (b) mimecan-null (KO) mice for the age groups 1 mo and 8 mo.

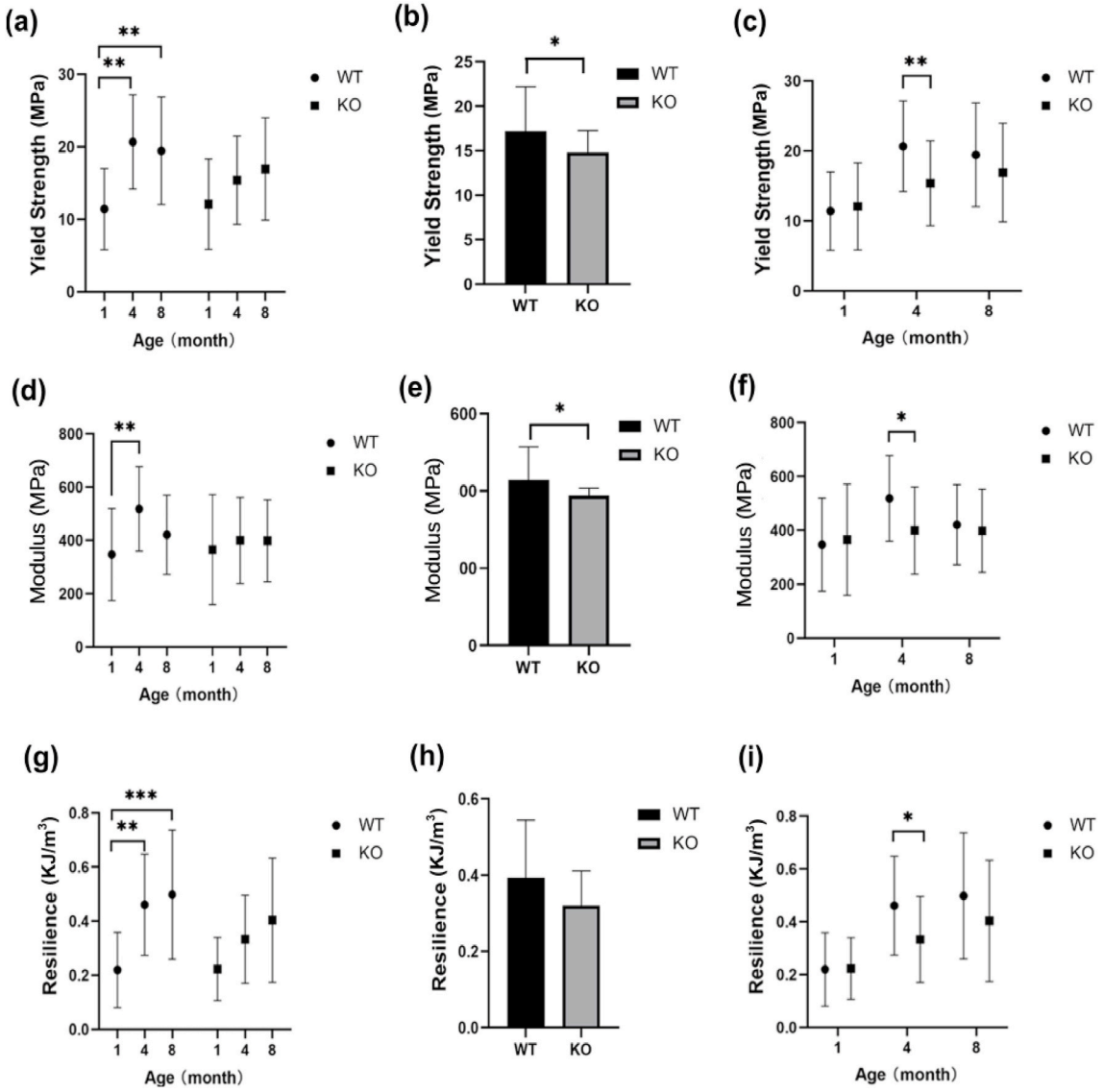

Fig. 4. Elasticity-related mechanical properties of wild-type (WT) and mimecan-null (KO) mouse tendon. Plots showing the effect of age and genotype are displayed for: (a, c) yield strength (d, f) modulus and (g, i) resilience. Overall effect of genotype (averaged for all tendons over all ages within the WT and KO groups) is also shown for the respective parameters in panels (b, e, h). Statistical significance is denoted at the following levels: * ($p < 0.05$), ** ($p < 0.01$), *** ($p < 0.001$). Error bars represent standard deviation. For informational purpose of reporting the model p-value for the interaction to justify moving on to the multiple comparisons, here the yield strength and modulus resulted in p-values of 0.02023 and 0.02331, respectively. (See Supplementary Information, Tables SI–1).

evaluated in Fig. 4 (c, f, i). A consistent lower mean value across all three elasticity parameters was observed in the KO group (squares) as compared to WT (circles) for the two older age groups, but this effect was statistically significant for only the 4-mo animals.

3.3. *Fracture properties*

The mean results of the fracture-related mechanical properties for each age point and genotype are listed in Table 1, and are displayed graphically in Fig. 5.

Graphs displaying the effects of age on WT and KO fracture properties are shown in Fig. 5 (a, d, g). For WT mice (circles), with the exception of fracture strain, significantly enhanced tendon fracture strength (Fig. 5(a)) and fracture toughness (Fig. 5(g)) were observed in older age groups compare to 1 mo animals. For KO mice (squares), this age trend was attenuated (Fig. 5 (a, g)), with the exception of fracture strain which revealed an increase in fracture strain from 1 mo to 4 mo mice (Fig. 5 (d)).

The overall effect of mimecan removal (i.e. pooling all tendon samples at all ages within each genotype) is seen in Fig. 5 (b, e, h), and shows a consistent decrease (i.e. mean value) across all three fracture parameters for KO mice compared to WT animals. However, when considering genotype and age as crossed factors, this reduction only met the threshold for statistical significance in the case of fracture strength (Fig. 5 (b)).

The effect of genotype is broken down by age group and statistically evaluated in Fig. 5 (c, f, i). A consistent lower mean value across all three elasticity parameters was observed in the KO group (squares) as compared to WT (circles) for the two older age groups, but this effect was statistically significance for the fracture strength and fracture toughness of only the 4-mo animals (Fig. 5 (c, i)).

4. Discussion

To the best of our knowledge, this preliminary work presents the first published investigation of mimecan knockout on tendon mechanical

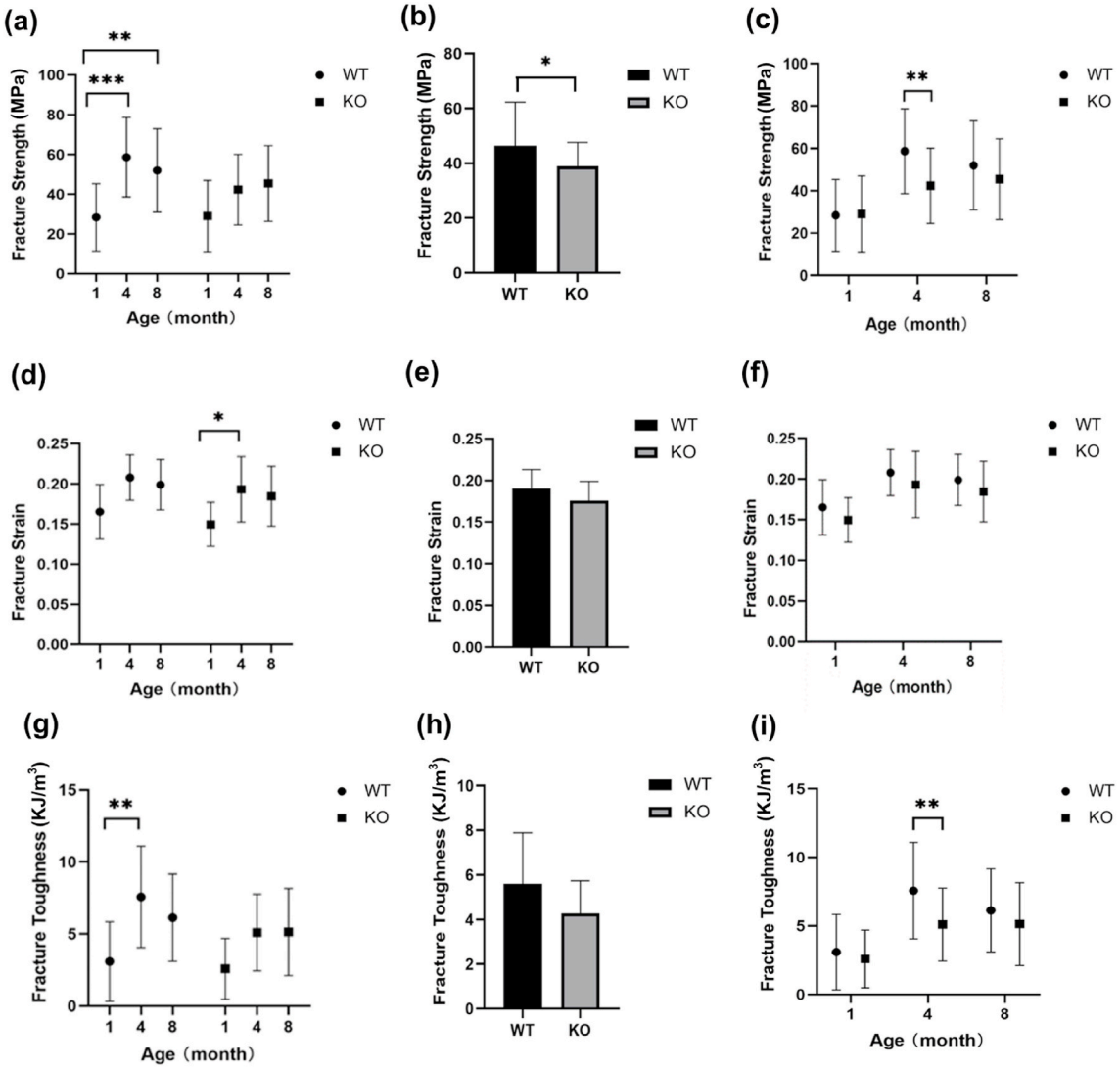

Fig. 5. Fracture-related mechanical properties of wild-type (WT) and mimecan-null (KO) mouse tendon. Plots showing the effect of age and genotype are displayed for: (a, c) fracture strength, (d, f) fracture strain and (g, i) fracture toughness. Overall effect of genotype (averaged for all tendons over all ages within the WT and KO groups) is also shown for the respective parameters in panels (b, e, h). Statistical significance is denoted at the following levels: * ($p < 0.05$), ** ($p < 0.01$), *** ($p < 0.001$). Error bars represent standard deviation. For informational purpose of reporting the model p-value for the interaction to justify moving on to the multiple comparisons, here the fracture strength resulted in a p-value = 0.01770. (See Supplementary Information, Tables SI–1).

properties. The main findings of the study were two-fold. Firstly, the absence of mimecan resulted overall in a more compliant mouse tail tendon (Fig. 4 (e)), as well as compromising the tissue's ability to resist yielding during elastic deformation (Fig. 4 (b)). Mimecan knockout also resulted in a generally weaker tendon (Fig. 5 (b)). Secondly, the overall effects of age on the mechanical properties, i.e. the enhancement of elasticity- and fracture-related parameters with age, as also found in previous studies (Goh et al., 2008; Goh et al., 2012; Goh et al., 2018), dominate in the tendons of normal mice, but this age trend was attenuated in the absence of mimecan, with the exception of fracture strain. (With regard to fracture strain, age has no overall effects on the mechanical property of tendons in WT mice but fracture strain increases from 1 mo to 4 mo in KO mice and remains unchanged thereafter.) In particular, all mechanical properties were significantly attenuated in 4 mo mimecan-null animals as compared to normal mice, with the exception of fracture strain (Panels (c), (f) and (i) in Figs. 4 and 5). (With regard to fracture strain, there was no significant difference in the mechanical property of tendons in KO versus WT mice across the 3 age points.)

Previous studies suggest that age-related enhancement of tendon mechanics is linked to changes in collagen structure and content. Whether the observed attenuation in the elastic and fracture properties resulting from mimecan knockout is being driven by some dysregulation in collagen assembly awaits further investigation. At bulk (i.e. tendon fascicle) level, absence of mimecan did not have a significant effect on the tendon fascicle diameter (as measured by light microscopy) across all age groups. Since stress is defined as the ratio of the force acting on the tendons to the tendon fascicle diameter, any change in the stress determined in this way could not be attributed to the bulk size. This suggests that changes at the next lower hierarchical level of tendon, e.g. collagen fibrillar level or tropocollagen molecular level, could have taken place. While mimecan studies in tendon are limited in the literature, proteomic investigations of equine tendon have hinted at a possible role of mimecan in regulating healthy tendon function, with a ~30-fold decrease in mimecan reported in old compared to young tendon (Peffers et al., 2014). Moreover, mimecan mouse knockout studies in other connective tissues have suggested that mimecan could be involved in regulating collagen fibrillogenesis during the early stages of an organism's development (Tasheva, 2002, Tasheva et al., 2002). Previous studies have shown how ECM structure influences the mechanical

function of tendons in the presence of ageing (Goh et al., 2008; Goh et al., 2012). Specifically, age-related enhancement of tendon mechanical parameters, notably modulus and fracture strength, are associated with increased collagen content (Goh et al., 2008; Goh et al., 2012).

A further observation of the current study was the shorter strain-softening region resulting from mimecan knockout (Fig. 3), which could be consistent with a reduction in the capacity of KO tendon fascicles to accommodate strain energy adsorption to fracture. The strain-softening region is influenced by the plasticity of the interfibrillar matrix (Szczesny and Elliott, 2014), suggesting that its curtailment in KO fascicles might lead to a reduction in plasticity compared to WT tendon. The capacity for strain-softening may be viewed as a fail-safe mechanism to minimise the catastrophic rupture of the fascicle. However, although the results showed a somewhat reduced strain energy adsorption to fracture in tendon fascicles in the absence of mimecan as compared to WT, this difference fell below the threshold for statistical significance (Fig. 5 (f)).

Connective tissues can exhibit hyper-elastic behaviour. Studies have evaluated the stress versus strain data obtained from the tensile test to rupture experiment of, e.g. nerve tissues, by fitting the data to hyper-elastic (mathematical) models such as Neo-Hookean, Yeoh and Ogden to determine the modulus-related coefficients (Fraser et al., 2021). Here, we chose to evaluate the elastic modulus identified from the point of inflexion on the stress-strain curve, as opposed to determining the coefficients from a hyper-elastic material model. The point of inflexion on the stress-strain curve is the maximum value of the elastic modulus; it underpins an assumption that the tissue undergoes a change from elastic to plastic state at the yield strain, which is identified with the point of inflexion. The application of this method in this study was prompted by previous studies on the elastic modulus of connective tissue from fascicles of the rodent tail tendon in e.g. decorin KO (Derwin and Soslowsky, 1999, Derwin et al., 2001; Robinson et al., 2004) and ageing mice (Goh et al., 2008; Goh et al., 2012). The method is straight-forward to apply and the results allow for useful comparison to the other studies, i.e.. decorin KO studies and ageing studies. We have chosen to use this approach as the simplest method to answer the question as to how the maximum rate of change in stress with respect to strain is affected by the absence of mimecan.

The current study was subject to a number of limitations. Firstly, with regard to the use of gene knockout animal models in general, it has been argued that the true effects of the knocked out gene could be masked by (1) potential compensatory mechanisms in knock-out animal models and (2) possible interactions between factors associated with developmental processes and those associated with eventual functions (Zhang et al., 2006). Such factors might then reasonably complicate the interpretation of experimental results. Given evidence that expression patterns of both mimecan (Peffers et al., 2014) and other SLRPs (Nomura, 2006) fluctuate with tendon age, possible compensatory changes in the expression levels of other SLRPs that may mitigate the effects of mimecan removal and partially recover normal tendon biomechanics during maturation in KO mice cannot be ruled out. Secondly, the number of mice available to the study was relatively low at between 3 and 5 per group. To achieve statistical robustness, we leveraged the 12 individual tendon fascicle segments per mouse tail as unique repeat measures in our mixed model analyses. Nevertheless, the current pilot study should be expanded to include a larger number of animals in future experiments that seek mechanistic insight. Thirdly, while the results of the present study support a potential role for mimecan in modulating collagen fibrillogenesis that could lead to changes in fibril structure and hence tendon mechanical integrity, no measurements of fibril ultrastructure (e.g. by transmission electron microscopy) were made in this pilot study. Imaging of ECM ultrastructure will form an important part of future, more comprehensive studies to ascertain possible structure-function mechanisms underpinning the mechanical compromise of mimecan-deficient tendon reported herein.

5. Conclusions

In conclusion we present, to the best of our knowledge, the first published study to show that mimecan gene-knockout can result in age-related changes in mouse tendon elasticity- and fracture-related properties. While these preliminary findings support a potential role for mimecan in the regulation of normal tendon mechanical function, further work is required to shed light on the mechanisms that underpin the current observations.

CRediT authorship contribution statement

C. Boote: Writing – review & editing, Methodology, Investigation, Formal analysis, Data curation, Conceptualization. **Q. Ma:** Writing – review & editing, Methodology, Formal analysis. **K.L. Goh:** Writing – review & editing, Writing – original draft, Validation, Supervision, Resources, Project administration, Methodology, Investigation, Formal analysis, Data curation, Conceptualization.

Declaration of competing interest

The authors declare that they have no known competing financial interests or personal relationships that could have appeared to influence the work reported in this paper.

Data availability

Data will be made available on request.

Acknowledgements

The authors thank Gary W Conrad and Elena S Tasheva of Division of Biology and College of Veterinary Medicine, Kansas State University, for the supply of the mice. Funding from the Cardiff University International Research Leave Fellowship Scheme (CB) and the China Scholarship Council Research Excellence Programme (QM, CB) is gratefully acknowledged. We are grateful to an anonymous reviewer for many helpful suggestions, particularly on the statistical analysis.

Appendix A. Supplementary data

Supplementary data to this article can be found online at https://doi.org/10.1016/j.jmbbm.2023.105672.

References

Bailey, A.J., Paul, R.G., Knott, L., 1998. Mechanisms of maturation and ageing of collagen. Mech. Ageing Dev. 106, 1–56.
Casroro, J.A., Berrelheim, A.A., Berrelheim, F.A., 1988. Water gradients across bovine cornea. Investig. Ophthalmol. Vis. Sci. 29, 963–968.
Chen, S., Birk, D.E., 2013. The regulatory roles of small leucine-rich proteoglycans in extracellular matrix assembly. FEBS J. 280, 2120–2137.
Derwin, K.A., Soslowsky, L.J., 1999. A quantitative investigation of structure-function relationships in a tendon fascicle model. J. Biomech. Eng. 121, 598–604.
Derwin, K.A., Soslowsky, L.J., Kimura, J.H., Plaas, A.H., 2001. Proteoglycans and glycosaminoglycan fine structure in the mouse tail tendon fascicle. J. Orthop. Res. 19, 269–277.
Dunkman, A.A., Buckley, M.R., Mienaltowski, M.J., Adams, S.M., Thomas, S.J., Satchell, L., Kumar, A., Pathmanathan, L., Beason, D.P., Iozzo, R.V., Birk, D.E., Soslowsky, L.J., 2013. Decorin expression is important for age-related changes in tendon structure and mechanical properties. Matrix Biol. 32, 3–13.
Ezura, Y., Chakravarti, S., Oldberg, Å., Chervoneva, I., Birk, D.E., 2000. Differential expression of lumican and fibromodulin regulate collagen fibrillogenesis in developing mouse tendons. JCB (J. Cell Biol.) 151 (4), 779–788.
Fraser, S., Barberio, C.G., Chaudhry, T., Power, D.M., Tan, S., Lawless, B.M., Espino, D. M., 2021. The effect of injurious compression on the elastic, hyper-elastic and visco-elastic properties of porcine peripheral nerves. J. Mech. Behav. Biomed. Mater. 121, 104624.
Funderburgh, J.L., Corpuz, L.M., Roth, M.R., Funderburgh, M.L., Tasheva, E.S., Conrad, G.W., 1997. Mimecan, the 25-kDa corneal keratan sulfate proteoglycan, Is a product of the gene producing osteoglycin. J. Biol. Chem. 272, 28089–28095.

Goh, K.L., Chen, Y., Chou, S.M., Listrat, A., Bechet, D., Wess, T.J.J., 2010. Effects of frozen storage temperature on the elasticity of tendons from a small murine model. Animal 4, 1613–1617.
Goh, K.L., Holmes, D.F., Lu, H.Y., Richardson, S., Kadler, K.E., Purslow, P.P., Wess, T.J., 2008. Ageing changes in the tensile properties of tendons : influence of collagen fibril volume. J. Biomech. Eng. 130, 021011.
Goh, K.L., Holmes, D.F., Lu, Y., Purslow, P.P., Kadler, K.E., Bechet, D., Wess, T.J., 2012. Bimodal collagen fibril diameter distributions direct age-related variations in tendon resilience and resistance to rupture. J. Appl. Physiol. 113, 878–888.
Goh, K.L., Holmes, D.F., Lu, Y.H., Kadler, K.E., Purslow, P.P., 2018. Age-related dataset on the mechanical properties and collagen fibril structure of tendons from a murine model. Sci. Data 5.
Goh, K.L., Hukins, D.W.L., Aspden, R.M., 2003. Critical length of collagen fibrils in extracellular matrix. J. Theor. Biol. 223, 259–261.
Goh, K.L., Listrat, A., Bechet, D., 2014. Hierarchical mechanics of connective tissues: integrating insights from nano to macroscopic studies. J. Biomed. Nanotechnol. 10 (10), 2464–2507.
Goh, K.L., Meakin, J.R., Aspden, R.M., Hukins, D.W.L., 2005. Influence of fibril taper on the function of collagen to reinforce extracellular matrix. Proc. Roy. Soc. Lond. B 272, 1979–1983.
Goh, K.L., Meakin, J.R., Aspden, R.M., Hukins, D.W.L., 2007. Stress transfer in collagen fibrils reinforcing connective tissues: effects of collagen fibril slenderness and relative stiffness. J. Theor. Biol. 245, 305–311.
Gordon, J.A., Freedman, B.R., Zuskov, A., Iozzo, R.V., Birk, D.E., Soslowsky, L.J., 2015. Achilles tendons from decorin- and biglycan-null mouse models have inferior mechanical and structural properties predicted by an image-based empirical damage model. J. Biomech. 48, 2110–2115.
Hukins, D.W.L., 1982. Biomechanical properties of collagen. In: Collagen in Health and Diseases, pp. 49–72.
Iozzo, R.V., Schaefer, L., 2015. Proteoglycan form and function: a comprehensive nomenclature of proteoglycans. Matrix Biol. 42, 11–55.
Jepsen, K.J., Wu, F., Peragallo, J.H., Paul, J., Roberts, L., Ezura, Y., Oldberg, A., Birk, D. E., Chakravarti, S., 2002. A syndrome of joint laxity and impaired tendon integrity in lumican- and fibromodulin-deficient mice. J. Biol. Chem. 277 (38), 35532–35540.
Kilts, T., Ameye, L., Syed-Picard, F., Ono, M., Berendsen, A.D., Oldberg, A., Heegaard, A.-M., Bi, Y., Young, M.F., 2009. Potential roles for the small leucine-rich proteoglycans biglycan and fibromodulin in ectopic ossification of tendon induced by exercise and in modulating rotarod performance. Scand. J. Med. Sci. Sports 19 (4), 536–546.
Lopez-Otın, C., Blasco, M.A., Partridge, L., Serrano, M., Kroemer, G., 2013. The hallmarks of aging. Cell 153, 1194-1127.
Nomura, Y., 2006. Structural change in decorin with skin aging. Connect. Tissue Res. 47 (5), 249–255.
Parry, D.A.D., Barnes, G.R.G., Craig, A.S., 1978. A comparison of the size distribution of collagen fibrils in connective tissues as a function of age and a possible relation between fibril size distribution and mechanical properties. Proc. R. Soc. Lond. Ser. B Biol. Sci. 203 (1152), 305–321.
Peffers, M.J., Thorpe, C.T., Collins, J.A., Eong, R., Wei, T.K.J., Screen, H.R.C., Clegg, P. D., 2014. Proteomic analysis reveals age-related changes in tendon matrix composition, with age- and injury-specific matrix fragmentation. J. Biol. Chem. 289 (37), 25867–25878.
Robinson, P.S., Lin, T.W., Reynolds, P.R., Derwin, K.A., Iozzo, R.V., Soslowsky, L.J., 2004. Strain-rate sensitive mechanical properties of tendon fascicles from mice with genetically engineered alterations in collagen and decorin. J. Biomech. Eng. 126, 252–257.
Schaefer, L., Iozzo, R.V., 2008. Biological functions of the small leucine-rich proteoglycans: from genetics to signal transduction. J. Biol. Chem. 283, 21305–21309.
Szczesny, S.E., Elliott, D.M., 2014. Incorporating plasticity of the interfibrillar matrix in shear lag models is necessary to replicate the multiscale mechanics of tendon fascicles. J. Mech. Behav. Biomed. Mater. 40, 325–338.
Tasheva, E.S., 2002. Analysis of the promoter region of human mimecan gene. Biochim. Biophys. Acta 1575 (1–3), 123–129.
Tasheva, E.S., Koester, A., Paulsen, A.Q., Garrett, A.S., Boyle, D.L., Davidson, H.J., Song, M., Fox, N., Conrad, G.W., 2002. Mimecan/osteoglycin-deficient mice have collagen fibril abnormalities. Mol. Vis. 8, 407–415.
Zhang, G., Ezura, Y., Chervoneva, I., Robinson, P.S., Beason, D.P., Carine, E.T., Soslowsky, L.J., Iozzo, R.V., Birk, D.E., 2006. Decorin regulates assembly of collagen fibrils and acquisition of biomechanical properties during tendon development. J. Cell. Biochem. 1449, 1436–1449.